Weak but uniform enrichment of the histone variant macroH2A1 along the inactive X chromosome.

Flore Mietton, Aditya Sengupta, Annie Molla, Gisele Picchi, Sophie Barral, Laurent Heliot, Thierry Grange, Anton Wutz, Stefan Dimitrov

Weak but uniform enrichment of the histone variant macroH2A1 along the inactive X chromosome

Mietton Flore [1] , Sengupta Aditya K. [2] , Molla Annie [1] , Picchi Gisele [3] , Barral Sophie [1] , Heliot Laurent [4] , Grange Thierry [3] , Wutz Anton [2] , Dimitrov Stefan [1] *

[1] *Institut d'oncologie/développement Albert Bonniot de Grenoble INSERM : U823, CHU Grenoble, EFS, Université Joseph Fourier - Grenoble I, Grenoble Cedex 9,FR*

[2] *Research Institute of Molecular Pathology IMP, Dr. Bohr-Gasse 7 A-1030 Vienna,AT*

[3] *IJM, Institut Jacques Monod CNRS : UMR7592, Université Denis Diderot - Paris VII, Université Pierre et Marie Curie - Paris VI, tour 43 2 place Jussieu 75251 PARIS CEDEX 05,FR*

[4] *IRI, Institut de Recherche Interdisciplinaire Université des Sciences et Technologies de Lille - Lille I, Université du Droit et de la Santé - Lille II , CNRS : FRE2963, FR*

* Correspondence should be adressed to: Stefan Dimitrov <Stefan.Dimitrov@ujf-grenoble.fr>

Abstract

In this work we have studied the enrichment and distribution of the histone variant mH2A1 in the condensed inactive X chromosome (Xi). By using highly specific antibodies against mH2A1 and stable HEK 293 cell lines expressing either GFP-mH2A1 or GFP-H2A, we found that the inactive X chromosome contains ~1.5 fold more of mH2A1 compared to the autosomes. To determine the in vivo distribution of mH2A1 along the X chromosome we used native ChIP on Chip technique. DNA, isolated from mH2A1 immunoprecipitated nucleosomes from either male or female mouse liver were hybridized to tiling microarrays covering either 5 kb around most promoters or the entire X chromosome. The data show that mH2A1 is uniformly distributed across the entire Xi. Interestingly, a stronger mH2A1 enrichment along the pseudoautosomal X chromosome region was observed in both sexes. Our results indicate a potential role for macroH2A in large scale chromosome structure and genome stability.

MESH Keywords Animals ; Cell Line ; Chickens ; Chromatin Immunoprecipitation ; Female ; Fluorescent Antibody Technique ; Histones ; metabolism ; Humans ; Liver ; metabolism ; Male ; Mice ; Nucleosomes ; metabolism ; Promoter Regions, Genetic ; genetics ; Protein Transport ; X Chromosome ; metabolism ; X Chromosome Inactivation

Introduction

In the eukaryotic cell nucleus DNA is packaged into chromatin. Chromatin exhibits a repetitive structure and its basic unit, the nucleosome, consists of an octamer of core histones (two each of H2A, H2B, H3 and H4) around which two superhelical turns of DNA are wrapped (35).

In addition to the conventional core histones, cells express histone variants. Such histone variants are non-allelic forms of the conventional histones and are expressed in a very low amount within the cell. The histone variants display varying degrees of similarity to their normal counterparts (34, 35). The most studied histone variants belong to the H2A and H3 families (7, 21, 30). When inserted into the histone octamer, variants may build nucleosomes with a different architecture and specialized functions (5, 7). For example, the crystal structure of the variant histone H2A.Z shows specific local molecular changes, which could affect the stability of the H2A.Z nucleosome particle (32). This could explain, in turn, the reported distinct properties of H2A.Z nucleosomal arrays in solution (1, 15, 16, 32). Recent data demonstrated that a novel histone variant, H2A.Bbd, is less tightly bound both in vitro and in vivo in the nucleosome compared to H2A (6, 17). The easier exchange and transfer of H2A.Bbd to a H3-H4 tetrameric particle could reflect the lower stability of the H2A.Bbd nucleosome (4, 17).

The histone variants play an important role in numerous vital cell processes as well as in several diseases (reviewed in 7, 21, 30, 37). For example, H2A.Z seems to be implicated in both activation and repression of transcription (13, 20, 22, 31). The reported data suggested that H2A.Z is also involved in chromosome segregation (29).

MacroH2A (mH2A) is an unusual histone variant, which consists of a domain similar to conventional H2A (H2A-like domain) fused to a large Non Histone Region (NHR) (26). mH2A reconstituted nucleosomes exhibit a modified structure with major alterations observed close to the dyad axis (3). These alterations interfere with the binding of the transcription factor NF-κB to its cognate sequence (3). In addition, SWI/SNF was unable to both remodel and mobilize mH2A variant nucleosomes. In vitro experiments showed that the presence of mH2A repressed Pol II transcription (14). It has also been reported that the presence of mH2A in the promoter results in a repression of transcription ex vivo (2, 25). In agreement with this, mH2A.1 is depleted on active genes and experiments with mH2A.1 (−/−) mice have shown that it is implicated in silencing of endogenous murine leukemia viruses (9, 10)

Several reports using immunofluorescence approaches have claimed that the inactive X chromosome (Xi) is enriched with the histone variant mH2A (8, 11, 12, 23). However, the specificity of the association of mH2A with the Xi was challenged since, by using the same immunofluorescence approach combined with GFP-mH2A localization and FRAP analysis, it was shown that the "enrichment" of mH2A may reflect the higher chromatin concentration within the inactive highly condensed X chromosome (27).

In order to solve this disagreement in the literature, we have studied the distribution of mH2A on Xi by using quantitative immunofluorescence and ChIP on Chip techniques. We found that the inactive X chromosome contains ~ 1.5 fold more mH2A1 compared to the autosomes. Intriguingly, mH2A1 shows uniform distribution all along the Xi.

MATERIALS AND METHODS

Cell culture and nuclei preparation

The human embryonic kidney HEK 293 cells were grown on Dulbecco's modified Eagle's medium. Media were supplemented with 10% foetal bovine serum (Biowhittaker, Europe).

Immunofluorescence experiments

Cells grown on glass coverslips were fixed at 37°C in 4% paraformaldhehyde, 2% sucrose and then permeabilized in PBS containing 0.2% Triton X100 for 15 min. Free binding sites were blocked with 0.5 mg/ml BSA and specific antibodies were then incubated for at least 30 min in PBS supplemented with 10% foetal bovine serum, 0.2% Tween-20 and 0.02% NaN_3. Unbound antibodies were removed by washing with PBS, 0.2% Tween-20 and specific staining was revealed with Alexa 546-conjugated antibodies (Interchim, France). DNA was visualized with DAPI. Images were collected with a ZEISS 510 Laser Scanning Confocal apparatus with a 40x immersion oil objective. Stable cell lines expressing GFP-mH2A1.2 or GFP-H2A were generated using standard methods.

Mononucleosome and oligosome preparation

Nuclei were isolated from mouse livers. After appropriate digestion of nuclei with micrococcal nuclease, linker histone-depleted chromatin (containing either mono- or oligosomes) was purified by centrifugation through sucrose gradients containing 0,6M NaCl. Then, the collected fractions were dialysed overnight against 50mM NaCl, 1mM EDTA, 10 mM Tris-HCl, pH 7.5 and if necessary concentrated on Centricon (DO_{260} varying from 2 to 6).

MacroH2A1 ChIP

Immunoprecipitation were carried out as follow: the linker histone depleted samples were incubated for 8h, at 4°C, with immunopurified macroH2A antibodies. Protein A- sepharose beads were first saturated with chicken erythrocyte nucleosomes (the anti-mH2A1 antibody we used does not recognize the chicken mH2A1) and then added to the mixture. The incubation lasted 1 hour under mild agitation, at room temperature. Then, beads were washed five times in 50mM NaCl, 1mM EDTA, 10 mM Tris-HCl, pH 7.5 and finally recovered for protein or DNA extractions. Mononucleosomes represent the input, the first IP wash corresponds to the unbound fraction while beads contain the bound material. An amount of each fraction was loaded onto a 12%–18% gradient SDS- PAGE and analysed by western blot. Successively histones macroH2A1 and H2A were detected on the same membrane. Nucleosomal DNA of each fraction was extracted from beads with a classical proteinase K digestion protocol.

Genome-wide mouse promoter DNA microarrays hybrydization

Genomic profiling was done by NimbleGen Systems as part of a Chromatin Immunoprecipitation Array Service. We used a mouse promoter tiling microarray set of two 385K arrays covering 5kb (about −4000 to +1000) of 24,939 promoters with a minimum spacing of 110 bp between probes excluding repeated sequences. Probes were 45 to 85 nucleotide-long with an isothermal design (target Tm: 76°C). We provided non-amplified DNA from input and pull-down (5 µg each) samples to NimbleGen Systems for differential labeling by random priming using a Cy3/Cy5-coupled 9mer oligonucleotide and hybridization to oligonucleotide arrays. For each experiment, input and pull-down channel signal intensities and scaled $\log_2$ ratios were provided by NimbleGen Systems. We then divided for each probe the immunoprecipitated over input ratio from the female liver chromatin with that from the male liver chromatin, and compared with t-tests the significance of the difference between the female to male ratio obtained with the X chromosome to that obtained with any autosome or the combination of all autosomes.

Hybridization on microarrays covering the whole mouse X chromosome

Microarray Design

Custom tiling microarrays were manufactured by NimbleGen Systems, Inc, based on a probe selection across provided by NimbleGen Systems Inc. The probes were selected to be unique within the mouse genome, at a median resolution of 306bp across the entire X chromosome and at a median resolution of 227bp for a part of chromosome 17 (4657287-19251247, NCBI m36). The microarray had 335514 probes from chromosome X and 52486 from chromosome 17. Note that repeated sequences were not present in the microarrays.

Hybridization

DNA was purified from macroH2A-enriched chromatin and input chromatin. Labeling (ChIP- red, input- green), hybridization to microarrays and data collection was performed by RZPD/ImaGenes.

Data Analysis

Signals from chromosome 17 were used for normalization and scaling within and across microarrays on the assumption that macroH2A distribution on chromosome 17 would be similar between males and females, unlike the X chromosomes. Tukey's biweight function was determined from M values ($\log_2$ ChIP/Input) from chromosome 17 signals of each array and subtracted from all M values for normalization. The mean absolute deviation of the M values across the normalized chromosome 17 signals in each array is used for scaling. A single array error model (19) was applied to calculate the confidence values and a weighted average was used to combine replicas for males and females respectively. In order to detect patterns within the data, the combined datasets were then transformed using wavelet smoothening to generate continuous wavelet transform heatmaps (33). Wavelet smoothened data at the 64-kb scale was obtained using maximal overlap discrete wavelet transform (MODWT) and used for analyses (33).

RESULTS

Quantitative immunofluorescence studies on the distribution of mH2A1

To study the association of mH2A with the inactive X chromosome we first developed a highly specific polyclonal antibody to mH2A1 (figures 1–3). The antibody was generated against the NHR of mH2A1. In whole HEK 293 cell extracts the immunopurified antibody recognizes a single polypeptide with a molecular mass of 42 kD, corresponding to mH2A1 (Figure 1A). We then used this antibody to study the distribution of mH2A1 in HEK 293 cells containing several inactive X chromosomes. The immunofluorescence analysis demonstrated that the antibody stained preferentially several dense regions of the interphase HEK 293 cell nucleus, called Barr Bodies, and corresponding to the inactive X chromosomes territories (Figure 1B). These observations are in agreement with the reported immunofluorescence data (8, 11). However, an enhanced DAPI staining of the Xi was also observed (Figures 1B and 2A). Since the enhanced DAPI staining is associated with a higher degree of compaction of Xi, even if mH2A1 is uniformly distributed all over the nucleus, one would expect a higher signal intensity with the anti-mH2A1 antibody of the Xi, which would reflect simply the higher degree of compaction (higher chromatin concentration) of Xi (for detail see 27). In agreement with this, in normal human female fibroblasts, all anti-conventional histone antibodies, as well as the anti-mH2A antibody, preferentially stained the inactive X chromosome (results not shown and (27). Moreover, both ectopically expressed GFP-mH2A and GFP-H2A were found concentrated on the inactive X chromosome (27). Thus, the observed preferential staining might reflect either an enrichment of mH2A1 or a higher chromatin concentration or both in the Xi.

To differentiate between these possibilities, we have carried out quantitative analysis of the amount of mH2A1 associated with Xi by using fluorescence microscopy and stable HEK 293 cell lines expressing either GFP-mH2A or GFP-H2A or naïve HEK 293 (Figure 2A). Note that these cells commonly exhibit several inactive X chromosomes (8). mH2A1 in the naïve cells was detected by using the anti-mH2A1 antibody (Figure 2A). The intensity of the fluorescence signals of the GFP and the anti-mH2A1 staining for the three types of cells was measured. The same measurements were also carried out for a randomly chosen region with the same dimensions as these of the Xi. The ratio of the two signals was then calculated and the same was done for the DAPI signals in the respective nucleus (Figure 2B). The data clearly show that this ratio for the DAPI staining is close to 1.5 in the three types of cells (Figure 2B). This demonstrates that in somatic cells the concentration of chromatin in the Xi is ~50% higher than that of autosomes. The ratio of the GFP fluorescence signals in the cells expressing GFP-H2A was also determined to 1.5, which further confirms, as expected, the higher concentration of chromatin in Xi and the accuracy of the DAPI measurements. The picture was different when we measured cells expressing green fluorescent protein tagged mH2A1. The ratio of the mH2A fluorescence signals from the Xi compared to autosomes in these cells was determined close to 2 (Figure 2B). Similarly, immunofluorescence staining of naive 293 cells with our mH2A antibody gave a nearly twofold higher signal intensity on the Xi compared to autosomes (Figure 2B). Therefore, mH2A shows higher enrichment on the Xi than would be expected from the calculated chromatin concentration. We conclude that the preferential staining of the Xi has two components; first an enrichment of mH2A1 and secondly it reflects a higher concentration of chromatin. Our data show that both components contribute essentially to similar extent to the observed signal over the Xi.

Distribution of mH2A1 on the promoters reveals uniform enrichment on the X chromosome in the liver of female mouse

Since mH2A1 might be involved in the repression of transcription, we first sought to detect whether enrichment on specific promoters could be detected. To test this we have carried out ChIp on Chip experiments by using DNA tiling microarrays covering 5 kb around the transcription start site of 25,000 mouse promoters (NimbleGen System Inc.) and oligonucleosomes prepared from male or female mouse liver that were immunoprecipitated with anti-mH2A antibody. DNA from the "input" and immunoprecipitated (bound) fraction was isolated and used for hybridization. We immunoprecipitated sufficient material to avoid amplification of the bound DNA, thus preventing biases due to PCR amplification.

Working with native nucleosomes preserves the mH2A1 epitopes and allows a very efficient ChIP (Figure 3, compare lanes 5, 6 and 7). The enrichment of mH2A in the immunoprecipitated (bound) fraction can be directly estimated by SDS gel electrophoresis and Western blotting of input and bound proteins. Firstly, Western blotting using the anti-mH2A1 antibody estimates the relative abundance of mH2A1 in the input and bound fractions (Figure 3). Secondly, using the same blot but with an anti-H2A antibody (Figure 3) the relative abundance of H2A in the input and bound fractions was estimated. The ratio between the mH2A1 and H2A signals is a measure of the enrichment of mH2A1 in the bound fraction. In the case of the bound fraction this ratio is much greater than 1, while for the input fraction the ratio was less than 1 (figure 3, compare lane 5 with lanes 1–4). This analysis confirms that a very high enrichment of mH2A1 in the bound fraction was achieved. The mH2A1 and H2A signals of the Western blots of the input fractions (figure 3, lanes 1–4) were used to generate calibration curves to allow calculation of the enrichment. In the different experiments we found between 8 and 15 fold enrichment of mH2A1 in the bound fraction compared to the input material.

The analysis of the promoter tiling arrays after hybridization did not detect mH2A1 enrichment on specific promoters on female relative to male liver, except for a cluster of repeated genes belonging to the Ott family (Figure 4A). With most probes within this area, the Ip/input ratio was consistently higher in the female than in the male. The Ott family corresponds to a clustered X-specific intrachromosomal repeat and most of the oligonucleotide probes within this region hybridized with a perfect match from 10 to 15 times to sequences repeated in close proximity on this portion of the X chromosome. As a consequence, the signal obtained with these probes was amplified, which could have allowed us to detect a weak and rather uniform mH2A1 enrichment that could have remained below detectable levels with the probes corresponding to single copy sequence. To detect such a weak enrichment, we compared the distribution of the signals obtained with all X chromosome probes with that of autosomal probes. When the immunoprecipitated over the input ratio for each probe of the female liver chromatin is divided by that of the male liver chromatin, the distribution of these ratios between the X and other autosomes can be directly compared using a Box plot representation (Figure 4B). This comparison revealed that there was a weak, but statistically highly significant mH2A1 enrichment ($p<10^{-230}$ using a t-test) on the female Xs compared to the male one. This enrichment was observed when the X was compared to any autosomes or to all autosomes together, whereas comparison of any autosome pair did not show such a difference (data not shown). Thus, indeed our interpretation that the repeated Ott cluster allowed to reveal a minor global enrichment of mH2A on the female X chromosomes appeared valid. Throughout the Ott cluster, we have not detected a higher enrichment at some specific positions relative to the transcription start site of the genes, suggesting that the mH2A enrichment at promoters is more global than specifically associated to promoter function.

Because the dynamic of the signal measured on microarrays tend to be always smaller than in the initial nucleic acid population, we aimed at obtaining an estimation of the enrichment factor of mH2A1 on the female X by comparing the enrichment ratio detected on the female to male bound/input ratio to that of the female to male input ratio normalized to the overall signal (Figure 4B). Since the X to autosome ratio in the female is twice that in the male, and the mH2A1 enrichment observed in the female is half the value observed for the normalized input, we estimate that there was about 1.5 fold higher levels of mH2A1 on the female Xs than on the male X. Assuming that the enrichment is due solely to the inactive X in the female, we estimate that there is at most twice more mH2A1 on the inactive X than on the active X.

Distribution of mH2A1 along the whole inactive X chromosome

Because we do not detect enrichment on specific promoter regions we next asked how mH2A1 is distributed along the inactive X chromosome. We have carried out a ChiP on Chip experiment using DNA tiling microarrays covering the entire mouse X chromosome (Figure 5). In order to be able to compare between different samples, particularly between males and female samples, we have included 15% of the probes on the array from chromosome 17. Assuming that macroH2A1 distribution is similar or invariant on chromosome 17 between the sexes, we normalized and scaled the data within and between arrays using these chromosome 17 probes (Figure 5). We observe a low, but rather uniform chromosome-wide enrichment of macroH2A1 on the female X chromosome, while the male X chromosome appears slightly depleted of macroH2A1 relative to chromosome 17 (Figure 5A, C). The low levels of enrichment may be in part because of the female cell has an active as well as an inactive chromosome, and presumably the active X of females is slightly depleted of macroH2A1 as in the single male X, thereby pulling down the averaged signal obtained from the inactive X. Some regions of the female X chromosome do not show the enrichment (Fig 5C

). These regions correspond to rodent-specific regions that are not conserved in other mammals (http://genome.ucsc.edu/), suggesting that they may have been acquired during evolution after establishment of the mechanism allowing mH2A enrichment. To note is that a relatively strong enrichment along the pseudoautosomal region (PAR) is observed in both sexes (Figure 5D).

DISCUSSION

In this work we have studied the origin of the higher staining of Xi with anti-mH2A1 antibody and the distribution of mH2A1 along the whole length of Xi by using quantitative fluorescence and ChIP on Chip approaches. The GFP- and immunofluorescence measurements show that the intensity of the mH2A1 staining of the Xi was ~twice stronger that this of the autosomes. This was associated with the higher condensation of the Xi as well as with an enrichment of mH2A1 in Xi, both effects exhibiting very similar contributions, i.e. about 50% of the enhanced staining was due to the Xi higher compaction and the remaining 50% reflected the preferential association of mH2A1 with the Xi. The ChIP on Chip experiments demonstrated that a higher proportion of mH2A1 was associated with the X chromosomes in female than in male liver along the whole length of the Xs, including promoters. This enrichment was most likely specific to the Xi based on the fluorescence analysis. Our quantitative analyses using these two types of approaches consistently revealed a 1.5 to 2 fold enrichment throughout the whole chromosome. Note that the antibody used showed a very low crossreactivity (not exceeding 10–15%) with mH2A2 and thus, the estimated higher amount of mH2A reflected only the enrichment of mH2A1 in Xi.

Since the function of mH2A is not well understood we could only hypothesize, at least for the moment, the meaning of our findings. mH2A appeared to be involved in transcriptional regulation. In vitro (14) and ex vivo (2) experiments pointed to an inhibitory role of mH2A in transcription. The depletion of mH2A1 in mice might regulate the expression of some genes (9) and appeared to be important for the silencing of endogenous murine leukemia viruses (10). The stable chromosome X inactivation requires, however, mH2A1 (18). Since no specific enrichment of mH2A1 on the promoter regions of the Xi genes was observed, the potential role of mH2A1 in Xi silencing should not involve a positioned nucleosome on the promoters as it was the case of B cells (2). Instead, we speculate that a mH2A1-dependent chromatin structure above the nucleosomal level could be involved in the X chromosome inactivation. The number of nucleosomes containing mH2A was estimated to be around 3% of the total number of nucleosomes and thus, bearing in mind the enrichment of mH2A1 on the Xi (the data presented in this work), close to 4–6% of the Xi nucleosomes should contain mH2A1. Thus, each 15^{th} to 25^{th} Xi nucleosome is a mH2A nucleosome. These mH2A nucleosomes, which are uniformly distributed on the Xi, could interact with some other factors and form some " coating" around the Xi and assist in its compaction and the maintenance of its inactive state. A potential candidate might be PARP-1. Indeed, PARP-1 was found associated in vivo with mH2A nucleosomes (24, 25) and it was shown that in vitro the association of PARP-1 promotes its condensation (36).

To note is that we have measured an enrichment of mH2A1 on the pseudoautosomal region (PAR) of both inactive and active chromosome X. This enrichment was higher than the bulk enrichment of mH2A1 on Xi. The PAR is the region where the X and Y chromosomes are homologous and homologous pairing of the XY body takes place during meiosis. This suggests that mH2A1 might be implicated in homologous recombination during meiosis. The assumption is that the small PAR of mice needs to generate one cross-over per meiosis and thus might have been selected for high recombination efficiency. Consequently, mH2A could be part of the machinery to silence these hyper-recombinogenic sequences to ensure genome stability in the soma. We predict that apart from gene regulation mH2A could be involved in suppressing chromosome recombination and thus serve a function in genomic stability.

Ackowledgements:

This work was supported by INSERM, CNRS and ANR Project no NT05-1_41978 and by the GEN-AU initiative of the Austrian ministry of science. S.D. acknowledges La Ligue Nationale contre le Cancer (Equipe labellisée La Ligue). We thank Drs. H. Fiegler and N.P. Carter for help in the initial stage of this work.

References:

- 1. Abbott DW , Ivanova VS , Wang X , Bonner WM , Ausio J 2001; Characterization of the stability and folding of H2A.Z chromatin particles: implications for transcriptional activation. J Biol Chem. 276: 41945- 9
- 2. Agelopoulos M , Thanos D 2006; Epigenetic determination of a cell-specific gene expression program by ATF-2 and the histone variant macroH2A. Embo J. 25: 4843- 53
- 3. Angelov D , Molla A , Perche PY , Hans F , Cote J , Khochbin S , Bouvet P , Dimitrov S 2003; The Histone Variant MacroH2A Interferes with Transcription Factor Binding and SWI/SNF Nucleosome Remodeling. Mol Cell. 11: 1033- 41
- 4. Angelov D , Verdel A , An W , Bondarenko V , Hans F , Doyen CM , Studitsky VM , Hamiche A , Roeder RG , Bouvet P , Dimitrov S 2004; SWI/SNF remodeling and p300-dependent transcription of histone variant H2ABbd nucleosomal arrays. Embo J. 23: 3815- 24
- 5. Ausio J , Abbott DW 2002; The many tales of a tail: carboxyl-terminal tail heterogeneity specializes histone H2A variants for defined chromatin function. Biochemistry. 41: 5945 - 9
- 6. Bao Y , Konesky K , Park YJ , Rosu S , Dyer PN , Rangasamy D , Tremethick DJ , Laybourn PJ , Luger K 2004; Nucleosomes containing the histone variant H2A.Bbd organize only 118 base pairs of DNA. Embo J. 23: 3314- 24
- 7. Boulard M , Bouvet P , Kundu TK , Dimitrov S 2007; Histone variant nucleosomes: structure, function and implication in disease. Subcell Biochem. 41: 71- 89

- 8.. Chadwick BP , Willard HF 2001; Histone H2A variants and the inactive X chromosome: identification of a second macroH2A variant. Hum Mol Genet. 10: 1101- 1113
- 9. Changolkar LN , Pehrson JR 2006; macroH2A1 histone variants are depleted on active genes but concentrated on the inactive X chromosome. Mol Cell Biol. 26: 4410- 20
- 10. Changolkar LN , Singh G , Pehrson JR 2008; macroH2A1-dependent silencing of endogenous murine leukemia viruses. Mol Cell Biol. 28: 2059- 65
- 11. Costanzi C , Pehrson JR 1998; Histone macroH2A1 is concentrated in the inactive X chromosome of female mammals. Nature. 393: 599- 601
- 12.. Costanzi C , Pehrson JR 2001; MacroH2A2, a new member of the macroH2A core histone family. J Biol Chem. 276: 21776- 21784
- 13. Dhillon N , Kamakaka RT 2000; A histone variant, Htz1p, and a Sir1p-like protein, Esc2p, mediate silencing at HMR. Mol Cell. 6: 769- 780
- 14. Doyen CM , An W , Angelov D , Bondarenko V , Mietton F , Studitsky VM , Hamiche A , Roeder RG , Bouvet P , Dimitrov S 2006; Mechanism of polymerase II transcription repression by the histone variant macroH2A. Mol Cell Biol. 26: 1156- 64
- 15. Fan JY , Gordon F , Luger K , Hansen JC , Tremethick DJ 2002; The essential histone variant H2A.Z regulates the equilibrium between different chromatin conformational states. Nat Struct Biol. 9: 172- 6
- 16. Fan JY , Rangasamy D , Luger K , Tremethick DJ 2004; H2A.Z alters the nucleosome surface to promote HP1alpha-mediated chromatin fiber folding. Mol Cell. 16: 655- 61
- 17. Gautier T , Abbott DW , Molla A , Verdel A , Ausio J , Dimitrov S 2004; Histone variant H2ABbd confers lower stability to the nucleosome. EMBO Rep. 5: 715- 20
- 18. Hernandez-Munoz I , Lund AH , van der Stoop P , Boutsma E , Muijrers I , Verhoeven E , Nusinow DA , Panning B , Marahrens Y , van Lohuizen M 2005; From the Cover: Stable X chromosome inactivation involves the PRC1 Polycomb complex and requires histone MACROH2A1 and the CULLIN3/SPOP ubiquitin E3 ligase. Proc Natl Acad Sci U S A. 102: 7635- 40
- 19. Hughes TR , Roberts CJ , Dai H , Jones AR , Meyer MR , Slade D , Burchard J , Dow S , Ward TR , Kidd MJ , Friend SH , Marton MJ 2000; Widespread aneuploidy revealed by DNA microarray expression profiling. Nat Genet. 25: 333- 7
- 20. Larochelle M , Gaudreau L 2003; H2A.Z has a function reminiscent of an activator required for preferential binding to intergenic DNA. Embo J. 22: 4512- 22
- 21. Malik HS , Henikoff S 2003; Phylogenomics of the nucleosome. Nat Struct Biol. 10: 882- 91
- 22. Meneghini MD , Wu M , Madhani HD 2003; Conserved histone variant H2A.Z protects euchromatin from the ectopic spread of silent heterochromatin. Cell. 112: 725- 36
- 23. Mermoud JE , Costanzi C , Pehrson JR , Brockdorff N 1999; Histone macroH2A1.2 relocates to the inactive X chromosome after initiation and propagation of X-inactivation. J Cell Biol. 147: 1399- 408
- 24. Nusinow DA , Hernandez-Munoz I , Fazzio TG , Shah GM , Kraus WL , Panning B 2007; Poly(ADP-ribose) polymerase 1 is inhibited by a histone H2A variant, MacroH2A, and contributes to silencing of the inactive X chromosome. J Biol Chem. 282: 12851- 9
- 25. Ouararhni K , Hadj-Slimane R , Ait-Si-Ali S , Robin P , Mietton F , Harel-Bellan A , Dimitrov S , Hamiche A 2006; The histone variant mH2A1.1 interferes with transcription by down-regulating PARP-1 enzymatic activity. Genes Dev. 20: 3324- 36
- 26. Pehrson JR , Fried VA 1992; MacroH2A, a core histone containing a large nonhistone region. Science. 257: 1398- 1400
- 27.. Perche P , Vourch C , Souchier C , Robert-Nicoud M , Dimitrov S , Khochbin C 2000; Higher concentrations of histone macroH2A in the Barr body are correlated with higher nucleosome density. Curr Biol. 10: 1531- 1534
- 28. Perry J , Palmer S , Gabriel A , Ashworth A 2001; A short pseudoautosomal region in laboratory mice. Genome Res. 11: 1826- 32
- 29. Rangasamy D , Greaves I , Tremethick DJ 2004; RNA interference demonstrates a novel role for H2A.Z in chromosome segregation. Nat Struct Mol Biol. 11: 650- 5
- 30. Redon C , Pilch D , Rogakou E , Sedelnikova O , Newrock K , Bonner W 2002; Histone H2A variants H2AX and H2AZ. Curr Opin Genet Dev. 12: 162- 9
- 31. Santisteban MS , Kalashnikova T , Smith MM 2000; Histone H2A.Z regulates transcription and is partially redundant with nucleosome remodeling complexes. Cell. 103: 411- 422
- 32.. Suto RK , Clarkson MJ , Tremethick DJ , Luger K 2000; Crystal structure of a nucleosome core particle containing the variant histone H2A.Z. Nature Struct Biol. 7: 1121- 1124
- 33. Thurman RE , Day N , Noble WS , Stamatoyannopoulos JA 2007; Identification of higher-order functional domains in the human ENCODE regions. Genome Res. 17: 917- 27
- 34.. Tsanev R , Russev G , Pashev I , Zlatanova J 1993; Replication and Transcription of Chromatin. CRC Press; Boca Raton, FI
- 35.. van Holde K 1988; Chromatin. Springer-Verlag KG; Berlin, Germany
- 36. Wacker DA , Ruhl DD , Balagamwala EH , Hope KM , Zhang T , Kraus WL 2007; The DNA binding and catalytic domains of poly(ADP-ribose) polymerase 1 cooperate in the regulation of chromatin structure and transcription. Mol Cell Biol. 27: 7475- 85
- 37. Zlatanova J , Thakar A 2008; H2A.Z: view from the top. Structure. 16: 166- 79

Figure 1

Preferential staining of mH2A1 in Xi of HEK 293 cells. **(A)** The anti-mH2A1 immunopurified antibody recognizes a single band with about 42 kD molecular mass within a HEK 293 cell extract. The same amount of HEK 293 whole cell extract was loaded on several wells of a 12% SDS gel. After completion of the electrophoresis the gel was cut and one part of the gel was stained with Coomassie blue (lane 2), while the other part was used for western blotting with anti-mH2A antibodies (lane 3). Lane 1, protein molecular mass marker. To note is that the same high specificity of the anti-mH2A1 antibody was also observed when extract from mouse cells was used (not shown). **(B)** The mH2A1 antibody detects the inactive X chromosome in HEK 293 cells at interphase. The top panel shows the nucleus of a HEK 293 cell stained with Hoechst and the low panel presents the immunostaining of the same cell with the mH2A1 antibody.

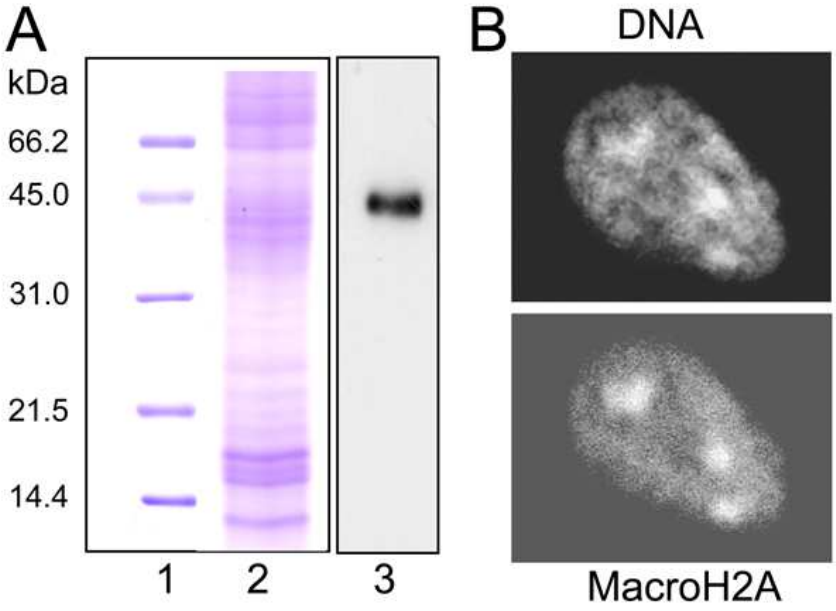

Figure 2

Measurements of the amount of mH2A1 associated with Xi in HEK 293 cells. HEK 293 cell lines, stably expressing either GFP-H2A or GFP-mH2A1.2, and naïve HEK 293 cells, were used to estimate the ratio of mH2A1/H2A in the Xi and the autosomes. To visualize mH2A1 in the naïve cells an immunopurified anti-mH2A1 antibody was used. (**A**) Preferential staining of the Xi with H2A-GFP, mH2A1-GFP and anti-mH2A1 antibody (first row). The second row shows the DAPI staining of the nuclei. The arrow indicates the Xi. (**B**) The inactive X chromosome is enriched of mH2A1. Images were deconvolved in 2D and then segmented with Metamorph software (Universal Imaging Corporation). The intensity of the fluorescence of the GFP and the anti-mH2A1 staining of the Xi in the three types of cells was measured. This was also done for a randomly chosen region of the nucleus with the same dimensions as these of the Xi and the ratio between the fluorescence intensities of the two signals was calculated in the respective cells. The same ratio was calculated for the DAPI signals. 80 either GFP-mH2A1.2 or GFP-H2A cells and 20 naïve HEK 293 cells were used in the experiments. The bar is the standard deviation.

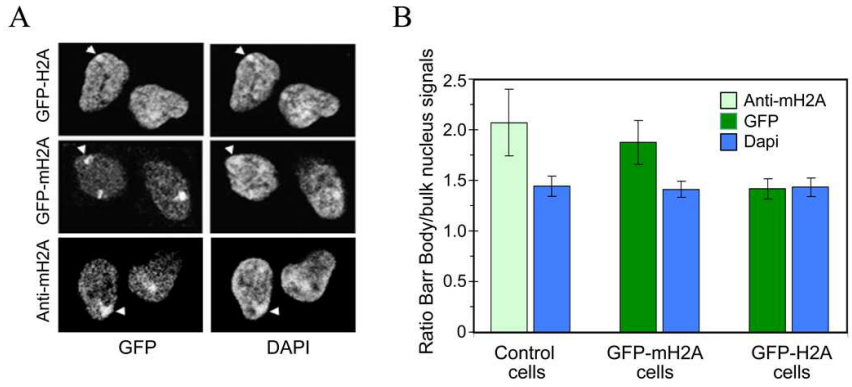

Figure 3

ChIP of mH2A1 nucleosomes. Nuclei, prepared from liver of female mice, were digested with micrococcal nuclease and mononucleosomes were purified on a sucrose gradient containing 0.6 M NaCl to remove linker histones. Mononucleosomes were immunoprecipitated by using anti-mH2A antibodies attached to protein-A agarose beads. Decreasing amounts of input nucleosomes (lanes 1–4, the nucleosome amounts of each successive lane is decreased twice), the bound (lane 5) and the unbound fractions (lane 6) were loaded on a 5–15 % gradient polyacrylamide gel, containing SDS. On lane 7 were loaded the control beads, which did not contain anti-mH2A antibodies, but that were incubated with the nucleosomes. After completion of the electrophoresis the proteins were transferred to a nitrocellulose filter. The filter was first revealed with a mH2A antibody and then with an anti-H2A antibody. Note that mH2A gives a much higher signal than H2A in the bound fraction (lane 5). In contrast, the mH2A signals of the input (lanes, 1–4) and the unbound (lane 6) fractions are much less than the respective signals for H2A.

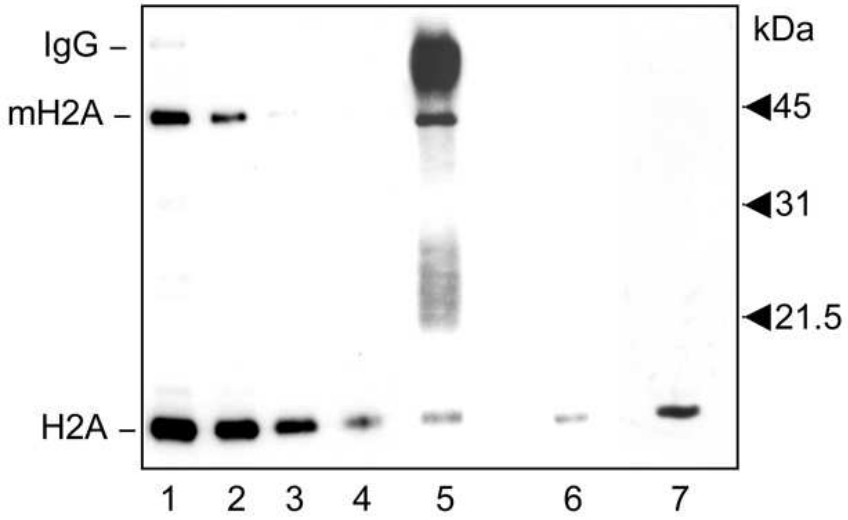

Figure 4

MacroH2A1 enrichment on the promoters of the X chromosome of female compared to male in mouse liver. Chromatin from both female and male mouse liver was immunoprecipitated with immunopurified anti-mH2A.1 antibody, and the input and bound DNA was used without amplification for hybridization on tiling arrays containing probes covering 5kb (about −4000 to +1000) of 24,939 mouse promoters. **(A)** Distribution of the log2 ratio of the Immunoprecipitated/Input signals on the promoter regions within a 6 Mb region encompassing the tandemly repeated Ott gene cluster. The top row shows genomic coordinates in Mb (UCSC mm5; NCBI build 33). The distribution of the signal that is generally centered around 0 is homogeneously shifted to higher values within the repeated region specifically in the female liver. **(B)** Comparative box plot analysis of the distribution of the mH2A enrichment levels in female relative to male on the different chromosomes. Both the female to male bound (Ip) to input ratio and the female to male normalized input ratio are represented (indicated at left and right side, respectively). Data from all pooled autosomes (Auto) are compared to that from the X alone. Very similar distributions are observed when any individual autosomes are analyzed.

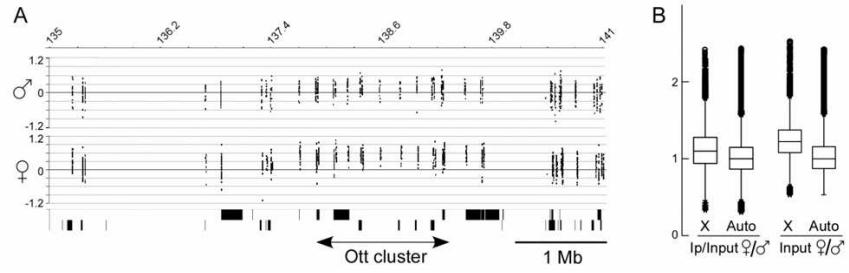

Figure 5

MacroH2A1 enrichment on the whole length of the X chromosome of female compared to male in mouse liver. Chromatin from both female and male mouse liver was immunoprecipitated with immunopurified anti-mH2A1 antibody, and the input and bound DNA (without PCR amplification) was used for hybridization on tiling arrays containing probes from the entire X chromosome and part of chromosome 17. M values ($\log_2$ IP/Input) were normalized to chromosome 17 using a weighted average (Tukey's biweight function). Arrays were scaled using mean absolute deviation of chromosome 17 values. (**A**) Comparative box plot analysis of the distribution of the mH2A enrichment levels in female and male on the 17th and X chromosomes. (**B–D**) Wavelet analysis (after (33)) was used to transform the combined ChIP-chip datasets in order to highlight broad patterns of macroH2A1 association on the chromatin. Wavelet smoothened data at the 64-kb scale was obtained using maximal overlap discrete wavelet transform (MODWT). The horizontal axes show genomic positions while the vertical axes show wavelet coefficient at that position at the 64-kb scale. The top row shows genomic coordinates (NCBI m36). (**B**) Chromosome 17 (4657287-19251247, NCBI m36). (**C**) X chromosome. MacroH2A1 enrichment is seen mainly across the entire female X compared to the male X. It should be noted that the signal on the female X is average of the contributions from both the active and the inactive X. (**D**) A high degree of macroH2A1 enrichment is seen in the pseudoautosomal region (28), starting from within the Fxy/Mid-1 gene (depicted with box, arrows show initiation sites of three annotated transcripts) of both the male and female X chromosomes.